

STALL COEFFICIENTS

Aerodynamic airfoil coefficients at large angles of attack

C. Lindenburg

This paper has been presented at the annual IEA symposium on the aerodynamics of wind turbines, December 4-5, 2000, NREL, CO, USA

JANUARY 2001

ABSTRACT

For the structural design of wind turbines the aerodynamic loads on the rotor blades must be known under all conditions. For parked conditions or the state with failed control mechanism, the wind can hit the blades with various angles of attack. From research for aerospace applications measured coefficients are available for angles of attack only up to stall. For larger angles of attack some empirical expressions are presented in this document, based on the assumption that the flow on one side of the airfoil is fully separated. The geometry of the upwind side of the airfoil is described in a limited set of parameters. With these parameters and with the aspect ratio of the complete rotor blade, empirical relations are obtained from measured data from various sources. These expressions are written in the program 'StC' which stands for Stall Coefficients.

1. INTRODUCTION

In 1995 Bjorn Montgomerie described empirical relations for the drag coefficients of an airfoil at 90 deg to the wind, [13]. Based on a similar approach, some empirical expressions are derived for the aerodynamic coefficients at large angles of attack. The basic assumption for this derivation is that the flow on one side of the airfoil is fully separated such that the airfoil can be approached by a curved plate. It is also assumed that for deep-stall flow the influence of Reynolds number is small for the range of wind turbine rotor blades. These expressions are written in a program called 'StC' which stands for Stall Coefficients.

For reversed flow, the aerodynamic coefficients are approximated with the lift and drag for an ellipsis with a radius equal to the nose radius of the airfoil.

The "90-deg drag" of the airfoils is also reduced for the finite length or "aspect ratio" of the rotor blades. The finite length gives a decay of the normal force towards the end or 'tip' of the blade. In 'StC' the effect of finite length is considered as a uniform reduction over the entire span.

2. EMPIRICAL FORMULATION

2.1 Drag Coefficient at 90 deg to the Wind

For deep stall some empirical relations of the aerodynamic coefficients are derived from aerodynamic coefficients of various sources. The different steps in the derivation are explained here, starting with the drag coefficient perpendicular to the flow.

2.1.1 Neglect the shape of the downwind side

In "Fluid Dynamic DRAG" of Hoerner [6] figure 33 on p.3-17 and figure 36 on p.3-18 give the drag coefficients of 2D objects with several elementary shapes, see figure 1. By comparison of objects with similar upwind shape in these figures, it is concluded that if the downwind side does not extend deep into the wake the shape of the downwind side has little or no effect on the flow and neither on the value of the drag coefficient.

2.1.2 Influence of the "wedge angles"

For a flat plate the drag coefficient is given in several references as:

Hoerner [6]: 1.98, Ostowari [14]: 2.06, Viterna [20]: 2.01.

For simplicity the drag coefficient in StC is chosen as $C_d(\text{flat}, 90) = 2$.

For 2D objects with sharp edges the flow leaves the object in the direction of these edges, which results in a lower drag compared to a long flat plate. From Hoerner, "Fluid-Dynamic DRAG" [6, p.3-18, fig.34], the drag of triangles with their corner upwind is fitted with $C_d = 1.98 - 0.4\phi - 0.16\phi^2$, see also figure 2. Here ϕ is one of the "wedge angles".

For airfoils the following expression is used in StC :

$$C_d = 2 - 0.2(\phi_{\text{nose}} + \phi_{\text{tail}}) - 0.08(\phi_{\text{nose}}^2 + \phi_{\text{tail}}^2).$$

In "Fluid Dynamic DRAG" [6, p.3-17, fig.33] Hoerner gives for the drag of a plate $C_d = 1.98$ and for the drag of a 45deg triangle $C_d = 1.55$. This reduction of 0.43 matches reasonably with the reduction of 0.413 following the expression given above.

2.1.3 Influence of the nose radius

For the trailing edge the direction in which the flow leaves the airfoil is well defined. The leading edge has a non-zero radius that may give some suction and lead the flow more downwind.

For an "oval-type" of edge-radius with a circular shape the drag is given by:

- Hoerner, "Fluid-Dynamic DRAG" [6, p.3-9, fig.13] (Re_{subcrit}):

$$C_d(\text{cylinder}) = 1.11 ;$$

$$C_d(\text{triangle, flat side upwind, } r_{\text{edge}}/h = 0.25) = 1.32 ;$$

$$C_d(\text{square, } r_{\text{edge}}/h = 0.02) = 1.55 .$$

- Hoerner; "Fluid-Dynamic DRAG" [6, p.3-17, fig.33],

$$C_d(\text{flat plate}) = 1.98 ;$$

$$C_d(\text{oval 1 : 2}) = 1.60 ;$$

$$C_d(\text{cylinder}) = 1.17 ;$$

$$C_d(\text{half - cylinder, upwind}) = 1.16 ;$$

$$C_d(\text{half - tube, upwind}) = 1.20 .$$

For the "oval-type" of edge radius, the drag coefficient fits more or less:

$$C_d = 1.98 (1 - 0.4(r_{\text{nose}} + r_{\text{tail}})/c) .$$

- ESDU 79026 [5, figure 6] gives drag coefficients of rounded triangles for $Re_{\text{subcrit}} = 1.5 \cdot 10^5$:

$r_{\text{nose}}/c = r_{\text{tail}}/c$	C_d
0.031391	1.94
0.0515	1.905
0.07578	1.785
0.10566	1.64

Probably because of the rear-body of these triangles, these drag coefficients do not apply the linearised relation, see figure 3.

The nose-radius of an airfoil approaches more an elliptical shape, for which ESDU 79026 [5, figure 8] gives the drag coefficients of ellipses at $Re_{\text{subcrit}} = 1.5 \cdot 10^5$:

t/c	$r_{\text{nose}}/c = r_{\text{tail}}/c$	C_d
1/10	0.005	1.83
1/5	0.02	1.77
1/4	0.03125	1.74
1/3	0.05556	1.70
1/2	0.125	1.60
1/1.8	0.15432	1.56
1/1.6	0.19531	1.51
1/1.4	0.2551	1.45
1/1.2	0.34722	1.35
1/1.0	0.5	1.2

For relatively flat ellipses the reduction in drag coefficient is stronger than for the "oval-type" of nose (and tail) radius and can be approached (a bit conservative) with $C_d = 2 - 1.08 \sqrt{r_{\text{edge}}/c}$, see also figure 3. Assuming a sharp trailing edge, the following expression is used in StC :

$$C_d = 1.7 + (0.3 - \phi_{\text{nose}} (0.2 + 0.08 \phi_{\text{nose}})) \cdot (1 - 1.8 \sqrt{r_{\text{nose}}/c}) - \phi_{\text{tail}} (0.2 + 0.08 \phi_{\text{tail}}) .$$

With this formulation the combined effect of nose radius and angle of the nose camber line is such that the influence of the nose camber-line decreases to zero if the nose radius exceeds $0.31c$.

For such a large nose radius, the shape of the leading edge is roughly cylindrical.

Also the influence of the nose-radius reduces to zero if the nose-angle ϕ_{nose} exceeds 60.4 deg, which is close to the separation point of a cylinder at $Re = 10^5$.

1.1.4 Influence of aspect ratio

In Hoerner "Fluid Dynamic DRAG" [6, p.3-16, fig.28] the drag coefficient is given as a function of aspect ratio AR. This is fitted by several authors:

Larry Viterna (AR<50) : $C_{d3D} = 1.11 + 0.018 AR$;

Björn Montgomerie : $C_{d3D} = 1.98 - 0.81 (1 - \exp(-20/AR))$;

Hibbs and Radkey (PROP) : $C_{d3D} = 1.98 - 0.81 \tanh(12.22/AR)$.

Compared to the measured values published by Hoerner, fig. 4, the expression of Hibbs and Radkey shows a good trend for very large aspect ratios but gives a small under-prediction for aspect ratios near 10. For StC a good and slightly conservative fit is found similar to the relation of Montgomerie: $C_{d3D} = 2.0 - 0.82 (1 - \exp(-17/AR))$.

Björn Montgomerie [13] also gives a description of the decay of aerodynamic drag towards the tip, based on a so-called "soap bubble" analogon. Because the tapered geometry of a rotor blade already differs from a rectangular flat plate, it is found premature to apply a drag-distribution.

In fact the nose radius and the wedge angles give a decrease in drag near the leading and trailing edges while the ends of the plate (or rotor blade) are still considered straight. Based on the fact that an angle of attack unequal to 90 deg also gives a reduction of the normal force, the so-called "effective aspect ratio" is introduced as $AR_{\text{eff}} = AR \cdot 2/C_n(\alpha)$. The factor 2 is the drag of a long flat plate. The expression for the 3D drag coefficient thus becomes

$$C_{d3D} = C_{d2D} (1 - 0.41 (1 - \exp(-17/AR_{\text{eff}}))) .$$

2.2 Aerodynamic Coefficients as Function of Angle of Attack

In the previous sections the 2D drag coefficient is described for cross sections that are perpendicular to the flow, for an angle of attack of 90 deg. In the following this coefficient is named $C_d(90)$.

2.2.1 Normal force coefficient

In "Fluid Dynamic LIFT" [7, p.21-1], Hoerner mentions that according to theory the normal force on the forward side of the plate is given by $C_n = 2\pi \sin \alpha / (4 + \pi \sin \alpha)$.

Following Hoerner, this is without the negative pressure on the rear side.

Including this negative rear-side pressure gives $C_n = C_d(90) \sin \alpha / (0.56 + 0.44 \sin \alpha)$.

For the effect of aspect ratio for various angles of attack an investigation is done to several formulations to combine the aspect-ratio effect and the distribution as a function of angle of attack. An expression that fits well with measured data is found to be

$$C_n = C_d(90) (1 / (0.56 + 0.44 \sin \alpha) - 0.41 (1 - \exp(-17 / AR_{\text{eff}}))) \sin \alpha .$$

2.2.2 Tangential force coefficient

Zero-lift angle in deep stall

Because of the suction at the rounded leading edge, airfoils do have some lift at 90 deg to the wind. Miley [11, figure 22], shows for NACA0015 at $Re = 1.23 \cdot 10^6$:

$$C_l(138) = -0.87 , \quad C_l(94) = 0.0 , \quad C_l(50) = 0.96 \text{ and } C_d(90) = 1.75 .$$

Note that for $\alpha = 50$ deg the flow differs too much from that for a flat plate.

(The maximum reversed lift coefficient is $C_l(171) = -0.80$.)

Other publications use an angle γ to express the lift: $C_l = C_n \cos(\alpha - \gamma)$

with $\gamma = 2$ to 4 deg. For small γ this can be written as $C_l = C_n (\cos \alpha - \sin \alpha \sin \gamma)$.

Because the angle γ is used to describe the suction at the leading edge it is expressed in terms of tangential force: $C_l = C_n \cos \alpha - C_t \sin \alpha$ where $C_t = C_n \sin \gamma$.

Based measured coefficients γ is fitted with $\gamma = 0.28 \sqrt{r_{\text{nose}}/c}$.

Viscous drag

Although it is a small contribution, the viscous tangential force coefficient is added considering that it acts on one side of the airfoil. The value of this tangential force is thus half the drag coefficient in laminar flow: $C_{t \text{ viscous}} = 1/2 \cdot 0.0075 \cos \alpha$.

For various angles of attack the tangential force is expressed as:

$$C_t = 1/2 \cdot 0.0075 \cos \alpha + C_n \sin \gamma .$$

The lift- and drag coefficients finally apply to:

$$C_l = C_n \cdot \cos \alpha - C_t \cdot \sin \alpha ;$$

$$C_d = C_n \cdot \sin \alpha + C_t \cdot \cos \alpha .$$

2.2.3 Moment coefficient

In ESDU 79026 [5] the chord-wise pressure position for ellipses with different thickness ratios is given as a function of angle of attack. For thickness ratios of 0.2 to 0.6 the pressure position with respect to the leading edge can be approximated accurately with

$$x_{cp} = 0.5 - (1 - \alpha/90) \cdot (0.175 + 0.13 (1 - \alpha/90))$$

Because an elliptical shape is a very rough approximation of an airfoil, only the part that is linear in $(1 - \alpha/90)$ is used for StC , which fits well for $\alpha = 45$ deg to $\alpha = 90$ deg:

$$C_m = -(0.25 - 0.175 (1 - \alpha/90)) C_n .$$

2.3 Reversed Flow

For the state of reversed flow, which differs from the deep stall flow because it is not completely separated, the aerodynamic coefficients are also sparse. For wind turbines that are parked (down-wind) with the blades pitched in vane position, the relative flow over the airfoils come from 180 degrees angle of attack. Because for strong winds most turbines are in a parked state, the static aerodynamic loads may dictate the design strength of the blade. Although the sharp trailing edge and the rounded leading edge of airfoils make it hard to describe the state of reversed flow, a very rough attempt is made to assess the aerodynamic characteristics. These characteristics are applied for angles of attack from 170deg up to 190deg.

2.3.1 Lift coefficient

Although airfoils are not symmetrical with respect to the chord line it is still considered that for reversed flow the angle of attack for zero lift is 180 deg.

In section 2.2.1 it was mentioned that Miley [11] gives for the NACA0015 section a maximum reversed lift coefficient of $C_l(171) = -0.80$. For a 12% thick airfoil section in reversed flow ($Re = 2 \cdot 10^6$) Hoerner gives a graph, [7, p.2-8, fig. 14], that shows a maximum lift coefficient of 0.8 at an angle of attack of 188deg. Based on these references it is concluded that for thin airfoils the maximum lift coefficient in reversed flow is always 0.8. For simplicity this maximum lift coefficient occurs at angles of attack of 190deg and 170deg, where in the latter case the lift coefficient is in fact -0.8. Based on the nose radius of the airfoil, the slope of the lift curve is calculated with a relation fitted to the characteristics of an ellipsis:

$$\partial C_l / \partial \alpha = 0.108 - 1.5 r_{\text{nose}} / c .$$

This relation is based Hoerner [7, p.2-7, fig.13] while α is expressed in degrees.

If this slope of the lift curve is too small to give a maximum lift coefficient of 0.8 at 190deg then the maximum "reversed lift coefficient" $C_l(190) = 10 (0.108 - 1.5 r_{\text{nose}} / c)$ is used.

1.3.2 Drag coefficient

The sharp trailing edge will probably cause a turbulent reversed flow. For an ellipsis in turbulent flow, Hoerner gives an expression for the drag coefficient as function of thickness ratio, [7, p.6-9]. Re-writing this expression as function of nose-radius gives:

$$C_d(180) = 0.005 (2 + \sqrt{2 r_{\text{nose}} / c} (4 + 240 r_{\text{nose}} / c)) .$$

For other angles of attack in reversed flow, the drag coefficient is calculated with

$$C_d(\alpha) = C_d(180) + 0.0003 (\alpha[\text{deg}] - 180)^2 .$$

2.3.2 Moment coefficient

The moment coefficient for reversed flow is calculated as if the lift and drag force act at the 75% chord location.







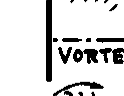




SHAPE	REF.	C_D
	—	1.17 _y
	(a)	1.20
	(g)	1.16
	(d)	1.60 _y
	(e)	1.55
	(a)	1.55
		1.98
	VORTEX STREET	
	(a)	2.00
	(a)	2.30
	(b)	2.20
	(a)	2.05 _y

Figure 1 Drag coefficients of various 2D objects, $Re = 10^4 \dots 10^6$ (from Hoerner, [6]).

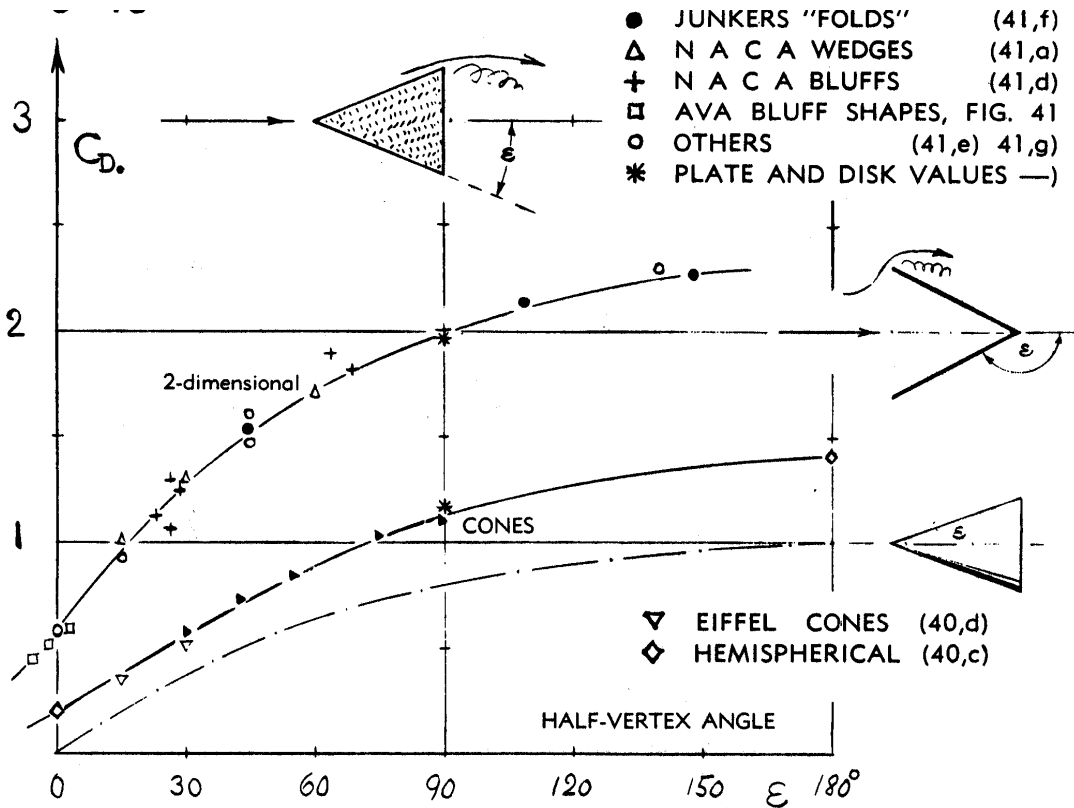


Figure 34. Drag coefficients of wedges, cones and similar shapes as a function of their half-vertex angle. At $\alpha = 90^\circ$ the shape is that of plates in normal flow; between 90 and 180°, "folds" and hollow cones are plotted with their opening against the oncoming stream.

Figure 2 Drag coefficients of blunt 2D wedges, $Re = 10^4 \dots 10^6$ (from Hoerner, [6]).

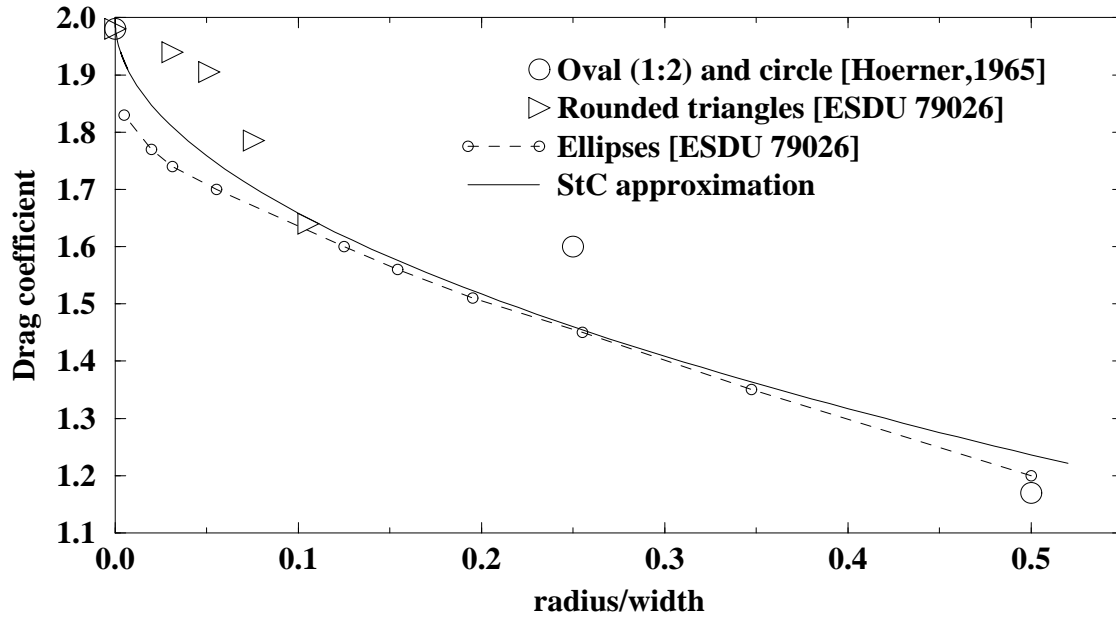


Figure 3. Drag coefficients of ovals and ellipses.

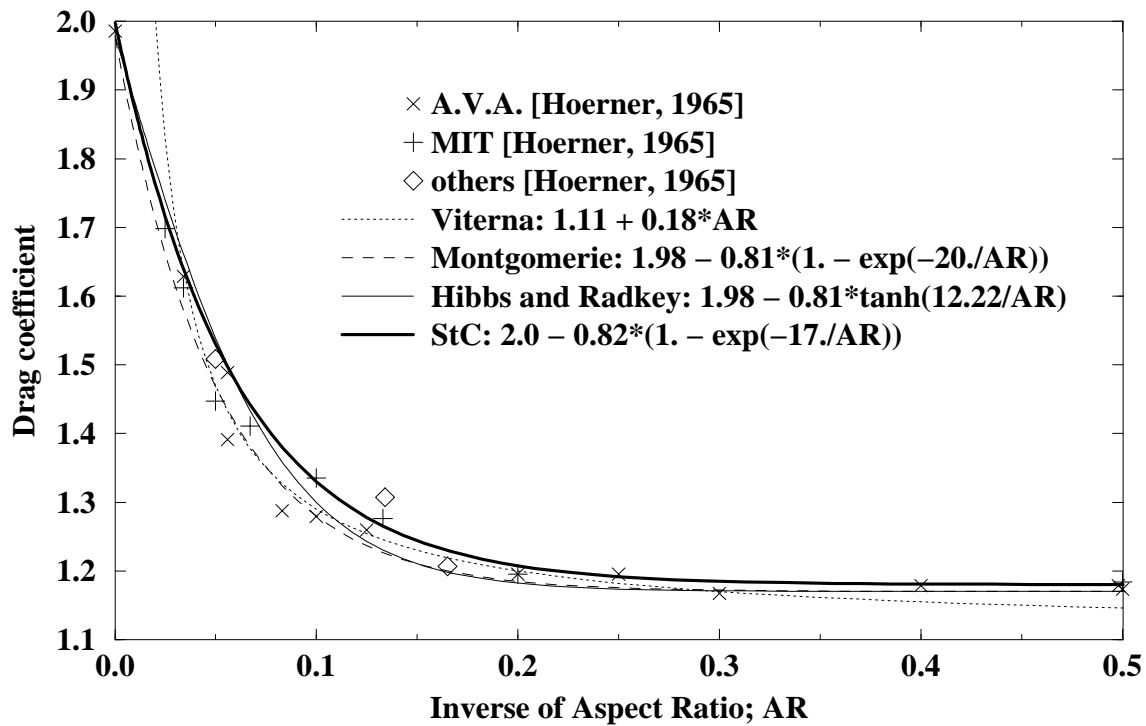


Figure 4. Drag of a rectangular plate as function of aspect ratio.

3. EVALUATION

3.1 Evaluation for Basic Geometrical Objects

For the drag of objects with a basic geometrical shape the drag coefficients do match because these objects are the basis of the empirical relations. Hoerner, [7, p.21-6], gives the drag coefficients for various flat and curved plates of finite aspect ratio:

Aspect Ratio	Camber	ϕ_{edge}	C_d	$\partial C_l / \partial \alpha$	$C_d(StC)$
0.2	0.0	0.0	1.20	-0.025/deg	1.207
1.0	0.0	0.0	1.16	-0.021/deg	1.180
5.0	0.0	0.0	1.20	-0.023/deg	1.207
5.0	-0.1	-0.395rad	1.22	-0.029/deg	1.282

Here the last column contains the predictions with StC . Although for the flat plates the aspect ratio effects are predicted well, it follows that the values calculated with StC for the curved plate show an over-estimation. Using the fact that the slope [rad^{-1}] of the lift curve is the opposite of the drag $C_d(90)$ gives for the drag coefficient of the curved plate $C_d = 0.029 \cdot 180/\pi = 1.66$ which is even larger than the predicted value.

In Hoerner, "Fluid-Dynamic DRAG" [6, p.4-6, fig.11], the drag of some "strut" sections between end-plates (with $AR = 10$ to 12) is given:

$$C_d(\text{flat plate}) = 1.97 ; \quad C_{dStC} = 2 ;$$

$$C_d(\text{"hook" angle, with "corner" upwind}) = 1.45 ; \quad C_{dStC} = 1.587 ;$$

$$C_d(\text{"hook" angle, with "corner" downwind}) = 1.72 ; \quad C_{dStC} = 2.108 .$$

Especially for the "hook" with the corner downwind the predictions with StC show an over-estimation because the rounded edges of these objects are not known and thus not modelled.

For a thin curved plate Bruining has measured the aerodynamic coefficients for various angles of attack at Reynolds numbers up to 200000, p.2.37- p.2.43 of [16].

	$C_{d \max}(90)$	$C_{l \max}$	$\alpha_{Cl \max}$
$Re = 0.1 \cdot 10^6$	1.927	1.364	30
$Re = 0.2 \cdot 10^6$	1.992	1.450	35 - 40
StC	2.133	1.245	39.1

Unfortunately the measured coefficients seem to depend on Reynolds number even at $\alpha = 90$ deg. The predicted maximum lift coefficient near 40 deg seems to be too small.

3.2 Comparison with Measured Coefficients

Aerodynamic coefficients for large angles of attack were found in several publications.

For 2D airfoil sections comparison of measured and calculated coefficients gives:

Airfoil	Ref.	$\alpha(C_1 = 0)$		$C_d(90)$		$C_{l,max}$		$\alpha(C_{l,max})$	
		meas.	StC	meas.	StC	meas.	StC	meas.	StC
NACA0012	[18]	92.54	92.05	2.09	1.902	1.11146	1.143	40.0	40.3
Idem, TDT tunnel		92.0	92.05	2.09	1.902	1.118	1.143	41.0	40.3
NACA0015	[11]	92.9	92.59	1.7	1.878	0.933	1.137	50.0	40.4
NACA4409	[14]	91.356	91.43	2.10	1.985	1.22	1.182	41.0	39.8
NACA4412	[14]	92.23	91.87	2.06	1.959	1.21	1.174	41.0	40.1
NACA4415	[14]	92.7848	92.30	2.068	1.933	1.2	1.166	40.0	40.4
NACA4418	[14]	92.097	92.73	2.06	1.906	1.17	1.157	40.0	40.5
NACA0012	[10]	92.63	92.05	2.05	1.902	1.171	1.143	42.0	40.3
NACA23012	[10]	92.33	91.78	2.082	1.948	1.217	1.166	40.0	40.1
NACA23017	[10]	92.55	92.40	2.078	1.902	1.152	1.149	45.0	40.4
FX 84-W-127	[10]	93.3	91.64	2.00	1.964	1.232	1.173	45.0	40.0
FX 84-W-218	[10]	96.4	92.63	2.04	1.939	1.152	1.175	45.0	40.5
LS-421 mod.	[10]	96.5	91.80	2.02	2.010	1.195	1.205	47.0	41.0
NACA23024	[12]	92.2	94.32	1.97	1.798	0.99	1.122	45.0	41.2
NACA63-215	[4]	92.0	91.97	1.98	1.959	1.094	1.176	45.0	40.2
GA(W)-1	[17]	90...	91.58	1.83	2.032	1.094	1.213	45.0	40.0
Idem. upside down		90...	91.56	1.72	1.794	1.094	1.082	45.0	-40.4

For airfoil sections with finite aspect ratio, comparison of measured and calculated coefficients gives:

Airfoil	Ref.	Asp. ratio	$\alpha(C_1 = 0)$		$C_d(90)$		$C_{l,max}$		$\alpha(C_{l,max})$	
			meas.	StC	meas.	StC	meas.	StC	meas.	StC
NACA0015	[2]	5.536	- - -	92.59	. . .	1.151	0.79	0.769	42.0	37.3
NACA4409	[15]	12	93.5	91.43	1.75	1.370	1.048	0.876	45.0	37.5
NACA4409	[15]	9	92.3	91.43	1.59	1.296	0.937	0.839	35.0	37.1
NACA4409	[15]	6	93.5	91.43	1.45	1.220	0.835	0.802	35.0	36.6
NACA4412	[15]	12	92.5	91.87	1.69	1.356	0.991	0.871	35.0	37.7
NACA4412	[15]	9	91.7	91.87	1.64	1.282	0.886	0.834	35.0	37.4
NACA4412	[15]	6	93.3	91.87	1.45	1.206	not	0.797		37.0
NACA4418	[15]	12	94.2	92.73	1.68	1.327	1.002	0.861	35.0	38.3
NACA4418	[15]	9	94.2	92.73	1.48	1.254	0.814	0.824	45.0	37.6
NACA4418	[15]	6	92.7	92.73	1.32	1.177	not	0.786		37.4
ClarkY	[16]	8	88.5	91.30	1.47	1.251	0.978	0.812	38.0	37.0
ClarkY	[11]	6	89.5	91.30	1.36	1.201	0.89	0.788	33.0	36.6

For the ClarkY airfoil the angle of attack for zero lift does not match well. A possible reason for this misfit can be that for the measurements the angle of attack is the angle with respect to the (nearly flat) pressure side of the ClarkY airfoil. The chord-line from trailing to leading edge of the Clark-Y airfoil makes an angle of about 2 deg with respect to the nearly flat pressure side, which is just the difference for $\alpha_{C_1=0}$.

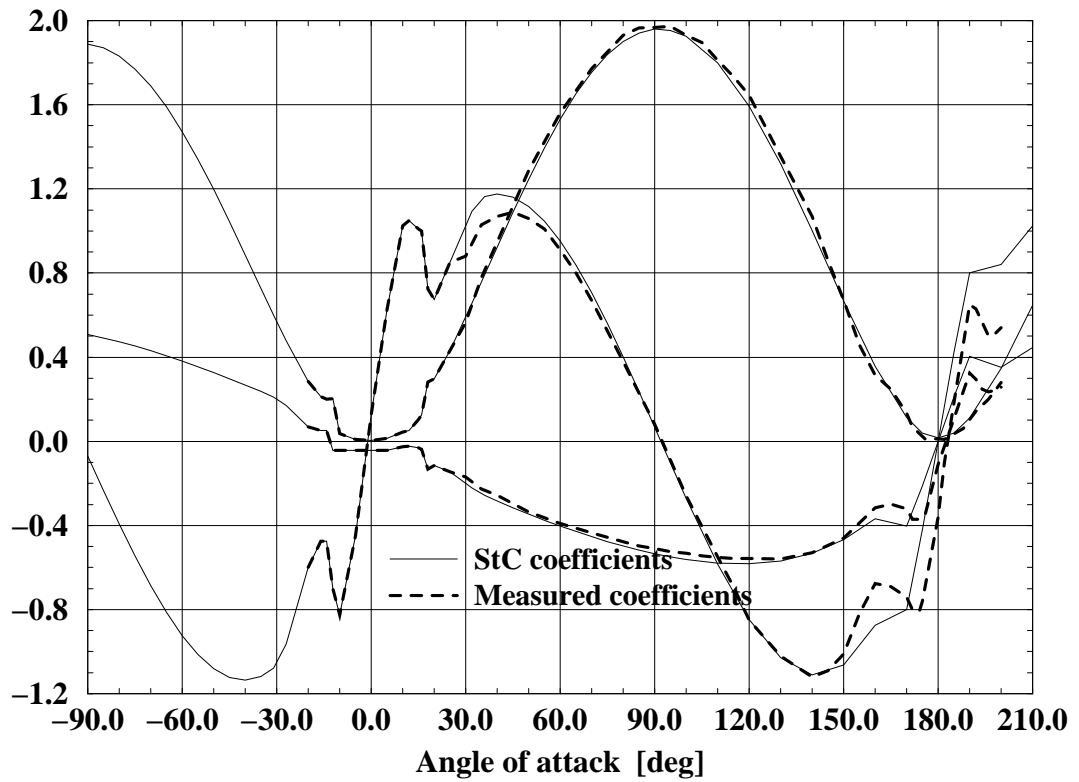


Figure 5. Coefficients for the NACA63-215 airfoil, infinite aspect ratio.

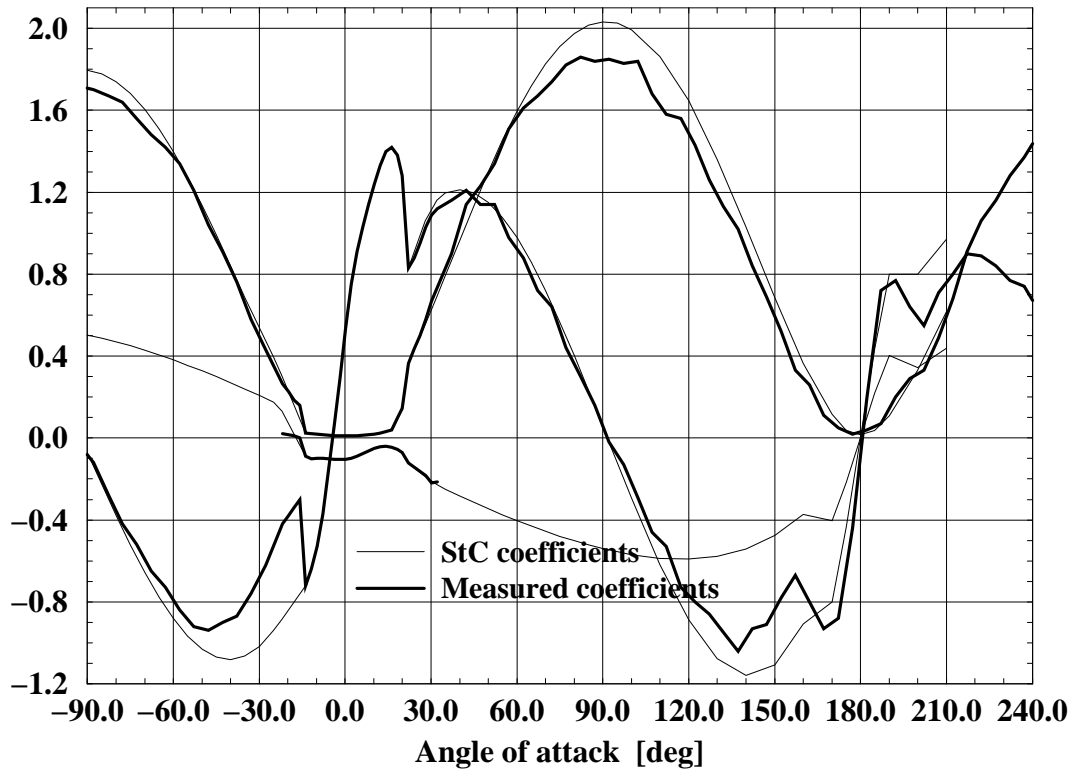


Figure 6. Coefficients for the GA(W)-1 airfoil, infinite aspect ratio.

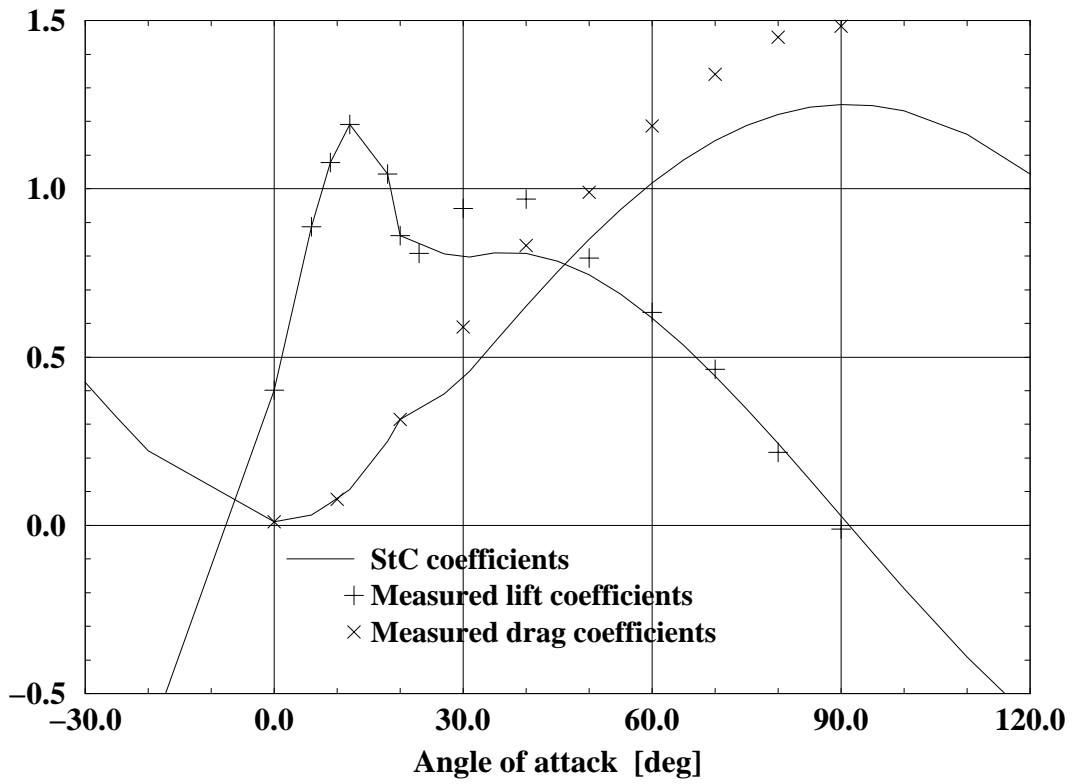


Figure 7. Coefficients for the Clark-Y airfoil, aspect ratio 8.

4. OPTIONAL IMPROVEMENTS

For possible improvements of the model for stall coefficients it is decided to include only the state of flow in which one side of the airfoil is in complete stall. This also reduces the dependency on the Reynolds number.

The following improvements are foreseen (November, 2000).

- The combination of aspect-ratio effect and the influence of angle of attack is still empirical. Some authors state that for finite aspect ratio, the drag coefficient for angles of attack near 90 deg (or between 45 deg and 135 deg) is independent of aspect ratio. In the PROP code Hibbs and Radkey use for the normal force coefficient the minimum value of $C_n(2D, \alpha)$ and $C_n(3D, 90deg)$. This gives remarkably higher values for the lift coefficients near 45 deg but also shows discontinuities.
Although measurements may have an absolute error from tunnel blockage (even when corrected) it is possible to use the ratio $C_{l_{max}}/C_{d_{max}}$ for further evaluation of this part of the *StC* model.
- For airfoils with a strong aft curvature the angle of attack (near 90 deg) for zero lift is under-predicted, which is the case for the FX 84-W-218 airfoil. In *StC* this is described with the angle γ which now only depends on the nose radius.
Extending the expression for γ with an expression including ϕ_{tail} may improve this part.
- Use different values of γ for angles of attack larger and smaller than 90 deg (also -90 deg). This can be used to describe the large suction peak at the leading edge for angles of attack smaller than 90 deg. The result will be that the predicted lift coefficient is not so much under-estimated.
- A more detailed description (if reasonably possible) for the coefficients near 180 deg.
A first improvement can be the "reversed" angle of attack for zero lift.
- Describe the position of the stagnation point as function of the geometry parameters.
This improves the moment coefficient.

Based on the fact that measurements may have errors from tunnel blockage, tunnel-wall interference etc. it may be that the absolute values for the deep stall coefficients have an error. If measurements are performed on asymmetrical airfoils for both large positive and large negative angles of attack, the difference between the resulting values are more useful for evaluation.

REFERENCES

- [1] Abbott, Ira H., and Von Doenhoff, Albert E.;
'*Theory of Wing Sections*'.
486-60586-8, Dover publications, Inc., New York, 1959.
- [2] Anderson, John D. Jr. (professor of Aerospace Engineering, Maryland);
'*FUNDAMENTALS OF AERODYNAMICS*'. second edition
ISBN 0-07-100767-9, McGraw-Hill, Inc, Singapore 1991.
- [3] Bak, C., Sorensen, N.N., Madsen, H.A. (Wind Energy and Atmospheric Physics Dept. Risoe National Laboratory, DK-4000 Roskilde, Denmark);
'*Airfoil Characteristics for the LM19.1 Blade Derived from 3D CFD*'.
Presented on "12-th Symposium on Aerodynamics of Wind Turbines", 1998.
- [4] Bloy, A.W. and Roberts, D.G.
(Department of Engineering (Aero). University of Manchester England);
'*Aerodynamic Characteristics of the NACA63₂-215 Aerofoil for Use in Wind Turbines*'.
In "Wind Engineering" Vol.17 No.2, 1993, pp.67-75.
- [5] ESDU;
'*Mean fluid forces and moments on cylindrical structures:
Polygonal sections with rounded corners including elliptical shapes*'.
Engineering Sciences Data Item Number 79026, ISBN 0 85679 274 8, 1979,
Specialised Printing Services Limited, 7-9 Charlotte Street London W1P 2ES.
- [6] Hoerner, Sighard F.;
'*FLUID-DYNAMIC DRAG, Practical Information on Aerodynamic Drag
and Hydrodynamic Resistance*'. Published by the author, 1965.
- [7] Hoerner, Sighard F. and Borst Henry V.;
'*FLUID-DYNAMIC LIFT, Practical Information on Aerodynamic and Hydrodynamic Lift*'.
Published by Mrs Liselotte A. Hoerner, 1968.
- [8] Lindenburg, C.;
'*STABLAD, Stability analysis Tools for Anisotropic rotor BLADE panels*'.
ECN-CX--99-013, (Confidential) Petten, June 1999.
- [9] Lissaman, P.B.S.;
'*Wind Turbine Airfoils and Rotor Wakes*'.
- [10] Massini*, G., Rossi*, E., D'Angelo**, S.
(*ENEA Rome, **Polytechnic University - Torin);
'*WIND TUNNEL MEASUREMENTS OF AERODYNAMIC COEFFICIENTS
OF ASYMMETRICAL AIRFOIL SECTIONS FOR WIND TURBINE BLADES
EXTENDED TO HIGH ANGLES OF ATTACK*'.
Contribution to European Wind Energy Conference, pp.241-245, June 6-10, 1988,
Herning, Denmark.
- [11] Miley, S.J.;
'*A Catalog of Low Reynolds Number Airfoil Data for Wind Turbine Applications*'.
RFP-3387 UC-60, Department of Aerospace Engineering, Texas A&M University,
College Station Texas 77843, February 1982.

- [12] Montag P. (DEWI);
'Untersuchung der Wirksamkeit von Wölbklappen an Windkraftanlagen im Vergleich zu Stall- and Pitch- geregelten Anlagen'.
 DEWI-V-940001, Deutsches Windenergie-Institut gemeinnützige GmbH, Wilhelmshaven, 1994.
- [13] Montgomerie, B.;
'DRAG COEFFICIENT DISTRIBUTION ON A WING AT 90 DEGREES TO THE WIND'. ECN-C-95-061, Petten, February 1996.
- [14] Ostowari, C.⁽¹⁾ and Naik, D.⁽²⁾
⁽¹⁾ Assistant Professor, ⁽²⁾ Graduate Research Assistant);
'Post stall studies of Untwisted Varying Aspect Ratio Blades with an NACA 4415 Airfoil Section - Part I'.
 In "Wind Engineering" Vol.8, No.3, 1984, pp.176-194.
- [15] Ostowari, C.⁽¹⁾ and Naik, D.⁽²⁾
⁽¹⁾ Assistant Professor, ⁽²⁾ Graduate Research Assistant);
'Post stall studies of Untwisted Varying Aspect Ratio Blades with NACA 44xx Series Airfoil Sections - Part II'.
 In "Wind Engineering" Vol.9, No.3, 1985, pp.149-164.
- [16] Petersen, H. (The Test Station for Windmills, Risoe National Laboratory, Denmark);
'Benchmark Test on Power Curve Computations on Wind Turbines - A Compendium'.
 Part 1, *Power Curve Computations* (Incomplete Draft, Nov. 86).
 Report of C.E.C. contract no. XVII/84/B/7033/11/004/17.
- [17] Satran, D. and Snyder, M.H.;
'Two-dimensional tests of GA(W)-1 and GA(W)-2 airfoils at angles-of-attack from 0 to 360 degrees'.
 Wind Energy Report No.1, January 1977. Wind Energy Laboratory, Wichita State University, Wichita, Kansas.
- [18] Strickland, J.H.
 (Assistant Professor, Mechanical Engineering, Texas Tech University, Lubbock, Texas);
'AERODYNAMICS OF THE DARRIEUS TURBINE'.
 In "Vertical-axis Wind Turbine Technology Workshop", SAND76-5586,
 Sandia Laboratories, Albuquerque, New Mexico 87115.
- [19] Timmer, W.A., Van Rooij, R.P.J.O.M. (TU-Delft);
'Airfoils at large angles of attack, The 2D-performance of DU 96-W-180 and DU 97-W-300 at large angles of attack'.
- [20] Viterna, L.A. and Janetzke, D.C. (NASA Lewis Research Center);
'THEORETICAL AND EXPERIMENTAL POWER FROM LARGE HORIZONTAL-AXIS WIND TURBINES'.
 In: "Fifth Biennial Wind Energy Conference & Workshop (WWV)", SERI/CP-635-1340,
 Sheraton Washington Hotel, Washington DC, 1981.